PROCEEDINGS, 48th Workshop on Geothermal Reservoir Engineering
Stanford University, Stanford, California, February 6-8, 2023
SGP-TR-224

Microcapsule Transport in Transparent Rough Fractures for EGS Fracture Modification

Pearl A. Tetteh, Brittney Seaburn, David Goering, John C. Stormont

University of New Mexico, Albuquerque, New Mexico, USA

patetteh215@unm.edu

Keywords: Microcapsules, transport, flow visualization, fracture aperture, blocking

ABSTRACT

Polymer-based injectates delivered by microcapsules are being evaluated as a means to modify fracture permeability to limit preferential flow that can lead to thermal short-circuiting. The microcapsules are sized so they enter only the larger, problematic fractures and rupture at elevated temperatures anticipated in the reservoir to deliver the polymer at the desired location. We report on experiments to understand microcapsule transport and determine the fracture size below which microcapsules are excluded from entry, i.e., the blocking function, for a rough fracture.

Flow visualization experiments were conducted to study the flow of microcapsules using water as the carrier fluid in transparent, horizontal rough fractures. The fracture characteristics (aperture, connectivity) was varied by both normal and shear displacement. A camera was used to record movement of the particles in the fractures. Microcapsule passage through, retention in, and exclusion from the fracture were measured. Image analysis methods were used to track microcapsule movement and interpret the amount of fracture blocking that occurs as a function of fracture characteristics and microcapsule size.

1. INTRODUCTION

Thermal short-circuiting in Enhanced Geothermal Systems (EGS) results in thermal breakthrough, decreased energy extraction efficiency, and reduced service life. Thermal short-circuiting is caused by preferential flow in relatively conductive fractures, which reduces the surface area available to transfer heat from the surrounding rock to the fluid (Patterson et al., 2020).

We are developing polymer-based materials that can be injected into fractures at targeted locations away from the wellbore to modify their permeability and consequently control the resulting flowrate through the fracture and the heat exchange with the formation. A schematic of the deployment of the polymer is shown in Figure 1. The polymer-based injectate is introduced into the fracture that is to be modified. The injectate is a mixture of four principal components: a polymer resin, a catalyst (i.e., hardener) to initiate polymerization, a pore-former (polyethylene glycol) and a high-temperature solvent that together will render the polymer porous. The catalyst, the pore former, and the solvent will be delivered in microcapsules that incorporate a clocking mechanism based on temperature so they are released at a target location away from the wellbore. The porous nature of the material will allow control on the resulting permeability of the fracture, and also prevents the treatment from completely sealing the fracture. Microcapsules are sized to prevent entry into smaller fractures so that the polymer formation is restricted to the larger fractures that are the target of the modification. Microcapsule rupture initiates as their temperature increases as the moving fluid is heated by the formation. The porous polymer begins to form and bond to the rock due to interaction of polymer resin, catalyst, and solvent.

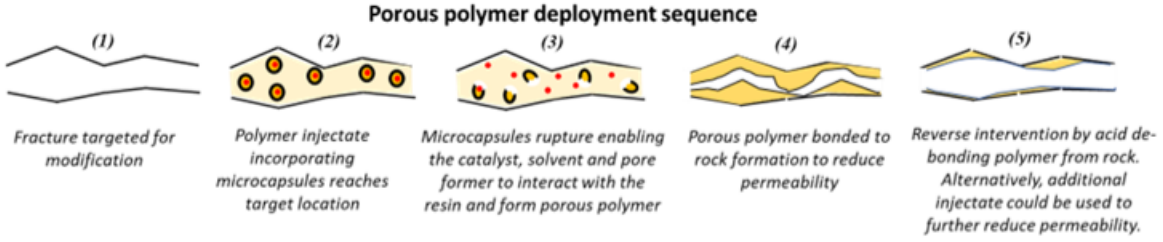

Figure 1 - Deployment sequence of a porous polymer to modify fracture permeability.

A key issue for the deployment of this technology is microcapsule movement in the fracture network. The microcapsules should be small enough to enter the targeted problematic fracture but large enough to be excluded from smaller fractures that do not require modification. We therefore seek to understand controls on microcapsule movement and define the blocking function, which is the relationship between microcapsule size and exclusion from a fracture.

Particle transport in fractures is relevant to many sub-surface applications, including proppant transport, smart tracers, and granular materials transport for lost circulation remediation. Previous work (Axelsson et al., 2009; Eklund and Stille, 2008) on proppant transport

and cement-based grout, respectively, concluded that the largest particle grain size should be 2 to 3 times lesser than the aperture size, and in some cases 5 times lesser to allow entry into the fractures. In a study of lost circulation materials, Lee and Dahi Taleghani (2020) found that bridging and blocking of a fracture was effective when the ratio of fracture size to particle size was 3.5. Microcapsule transport in fractures is known to be affected by their density relative to the carrier fluid (Roy et al., 2015). Movement of particles in fractures has often been focused on settling behavior of the relatively dense particles; however, for our application, we anticipate that the microcapsules and the carrier fluid will have nearly equal densities and therefore gravity settling will not be a concern in their movement.

In this paper, we present preliminary results from an experimental set-up used to visualize microcapsule movement in rough-walled fractures. A transparent rough-walled fracture replica that can be displaced normally and sheared was used to create fractures with different characteristics. The hydraulic aperture of the fractures was first measured using water. Microcapsules of different sizes were then transported with water as the carrier fluid through the fractures. Images obtained during flow were used to interpret the blocked area of the fracture and track particle movement in the fracture.

2. MATERIALS AND METHODS

A fracture flow visualization system was developed to obtain data on flow and blockage in rough-walled fractures. The system consists of a transparent fracture, a manifold to introduce fluid into the fracture, tubing that connects the fracture system to a source containing the mixture of microcapsules and water, a peristaltic pump, an ultraviolet light source, and a camera (Figure 2).

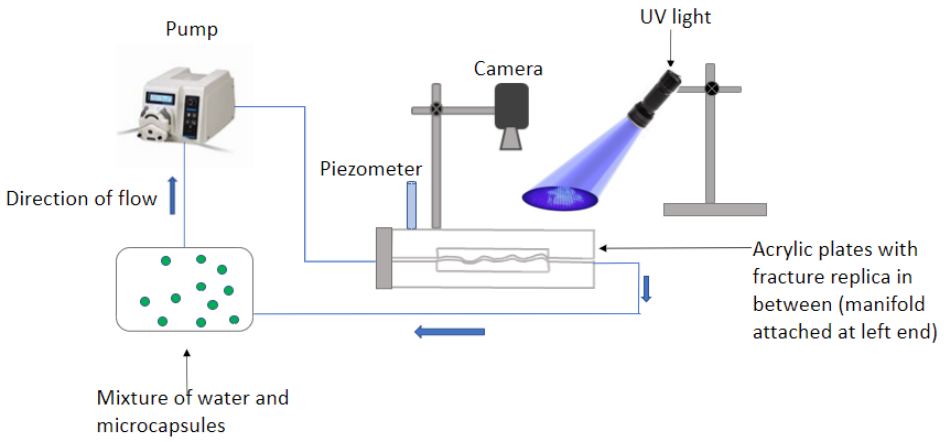

Figure 2 - Schematic diagram of the flow visualization set-up.

The transparent fracture replica with dimensions 85 mm by 100 mm was constructed from a natural granite fracture. A mold was first made from casting silicon against the granite fracture. Clear resin was then cast in the mold to create the fracture replica. The transparent fracture replica was placed between two clear acrylic plates for support. The fracture can be shimmed to produce normal displacement of the fracture, and/or displaced laterally to produce a shear fracture.

The fracture topography was measured using a mechanical profiler, an autonomous system that measures the height of the surface at pre-programmed intervals to generate a 3D representation of the fracture surface. The fracture asperity height (the z-direction) of the acrylic fracture replica was collected every 0.38 mm in the x-direction and 0.5 mm in the y-direction. The Joint Roughness Coefficient (JRC) of the fracture was found to be 3.92.

The fracture was sealed along the sides with neoprene and adhesive to avoid leakage of the water. The fracture replica was connected to a manifold to introduce the mixture of water and microcapsules at one end, the other end drained to atmospheric pressure. A pump was used to circulate water with the microcapsules through the fracture. Tests were conducted at room temperature.

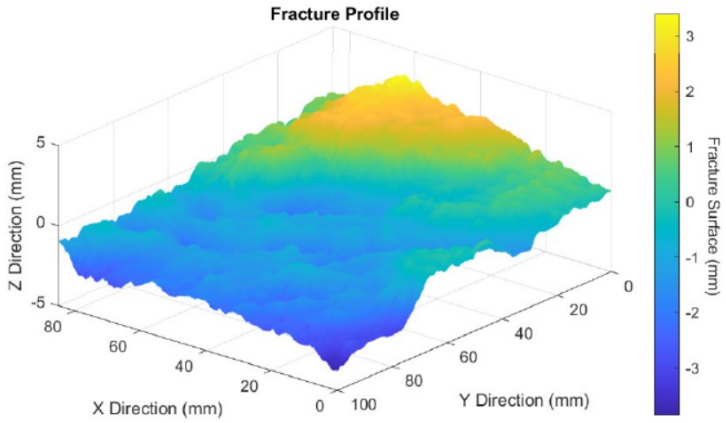

Figure 3 - Topographic map of fracture used to create aperture map when fracture was sheared differently.

A piezometer tube was integrated into the acrylic replica on the upstream side to measure the upstream head. The difference in the piezometer level on the upstream end and downstream elevation was used to obtain the head lost across the fracture. The flow rate from the pump was confirmed by collecting water on the downstream end for a period of time. The hydraulic aperture was interpreted from the measured pressure drop and flow rate during steady-state flow using the so-called cubic law (Witherspoon et al., 1980).

The microcapsules were fluorescent microspheres made from polyethylene. There were two sets of microcapsules sized 0.85 mm-1 mm and 0.5 mm with the equal density 1g/cm^3, same as the carrier fluid (water).

For a given fracture displacement (normal or shear), the hydraulic aperture of the fracture was first measured using only water. Microcapsules were then introduced into the water and the mixture was delivered to the fracture. Circulating, steady-state flow was continued for 15 minutes or until blockage completely prevented flow of microcapsules through the fracture.

A camera above the fracture was used to capture images during the flow of microcapsules for data interpretation. A UV light source was used above the set up to enable image capturing of the fluorescent microcapsules during the tests. Video during flow was used to produce tracks of particle movement using the TRACTRAC software. An image at the end of the test was used to obtain the percentage and area of fracture blocked through an image analysis program developed in MATLAB.

The fracture topography data was used to create a model for the aperture field that results from shear displacement. The fracture aperture field is shown for different amounts of shear displacement in Figure 3. These results reveal that shear displacement creates complicated fracture networks that vary significantly with the amount of shear, consistent with the findings of others (Naets et al., 2022).

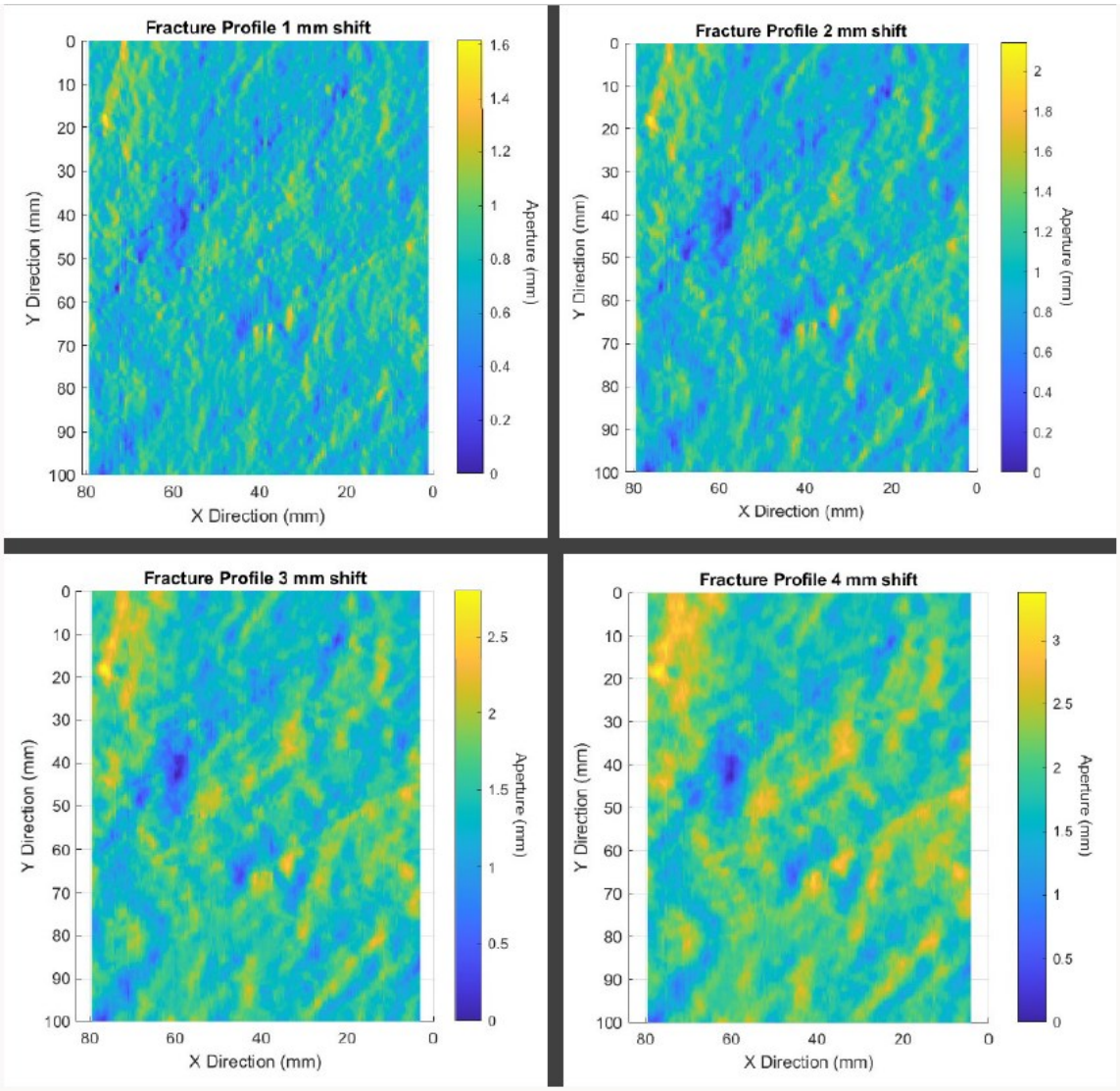

Figure 4 – Map of fracture apertures for 4 different amounts of shear displacement.

3. RESULTS

3.1 Tests on Normally Displaced Fractures

Photographs taken at the conclusion of the test (Figure 4a) were converted to high contrast images (black and white as shown in Figure 4b). In the black and white images, the white areas are the microcapsules. The amount of the fracture area covered by microcapsules (blockage) is calculated through the image analysis program developed in MATLAB.

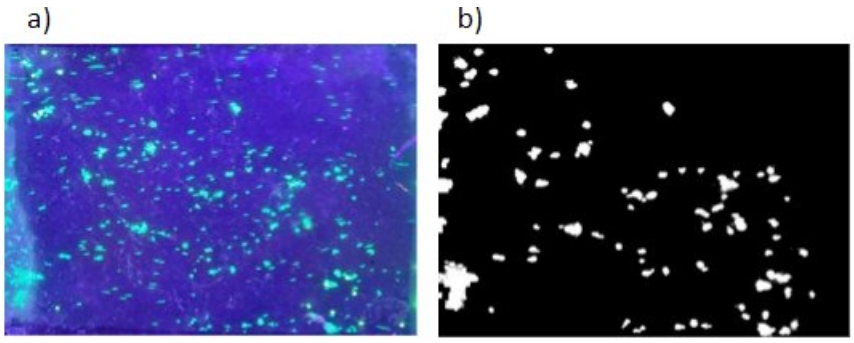

Figure 5 - Image at conclusion of 15 minutes of steady state flow of 0.5 mm diameter microcapsules through a 0.9 mm normally displaced rough-walled fracture. Image (a) Original photo from flow test, image (b) High contrast image derived from photograph including removal of noise. White areas are microcapsules that are retained in fracture, and thus block flow. The calculated blocked area is 6%

In Figure 5 below, we plot the percent of the fracture area that was blocked with 0.5 mm microcapsules as a function of the ratio of the aperture size (normal displacement) to the microcapsule size. These preliminary results indicate that significant blocking (as defined blockage of 10% or more of the flow path area) does not occur until the relative size of the fracture is much less than 2, which is a smaller value than many existing conventional blocking criteria developed for other materials under different conditions. This suggests that microcapsule size will need to be quite close to or larger than the fracture aperture in order to be excluded (blocked) from a fracture.

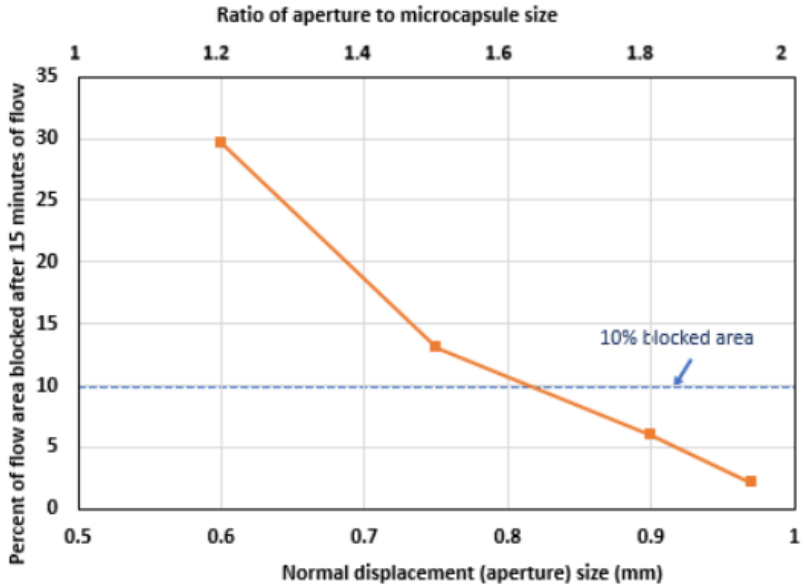

Figure 6 - Results from flow visualization experiments on normally displaced fractures.

3.2 Tests on Sheared Fractures

Tests on sheared fractures resulted in more complex flow behavior. In some cases, flow through the sample was blocked completely. Figure 6 shows a fracture aperture map overlain with an image from the conclusion of the test. Prior to introducing 1 mm diameter microcapsules, the hydraulic aperture of the fracture was measured as 0.89 mm at 2 mm of shear displacement. The map shows regions with sizes less than 1 mm in blue, and regions with an aperture larger than 1 mm in white. Microcapsules penetrated the fracture but did not make it through as a continuous flow network could not be established even though there were other areas of the fracture with apertures larger than the microcapsules.

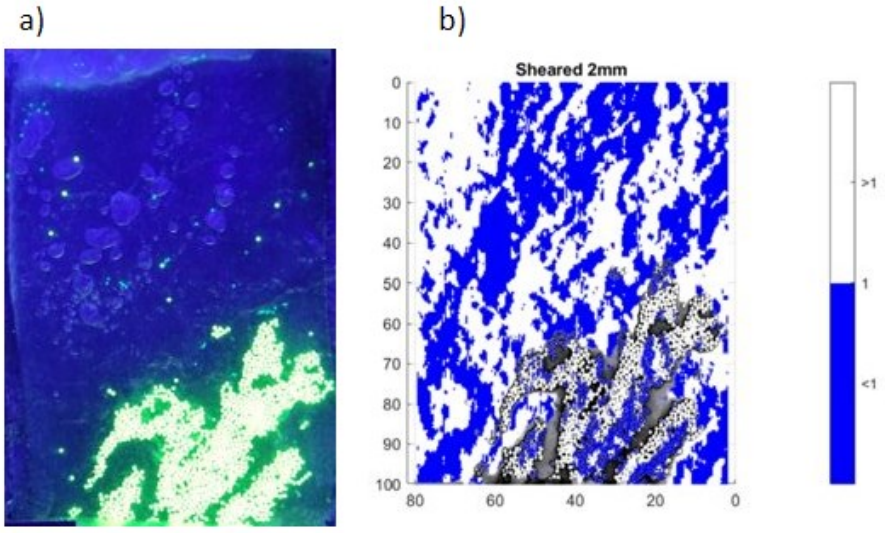

Figure 7 – (a) Photograph at conclusion of test that resulted in complete blockage of the fracture. The 1 mm diameter microcapsules were introduced at the bottom of the photograph. (b) Image derived from photograph overlain on fracture aperture map.

In shear tests when steady flow of microcapsules was established through the fracture, the trajectory of the flow paths of the microcapsules was no longer straight as it was for the normally displaced fractures (Figure 7). Figure 8 shows results from the same test used to derive Figure 7b (1 mm diameter microcapsules in fracture that was sheared 3 mm and a 1.2 mm hydraulic aperture). Figure 8a is a photograph of the fracture at the conclusion of the test which reveals considerable blockage. In Figure 8b, the particle trajectories are shown near the conclusion of the test, and reveal that flow was concentrated into channels and excluded from large portions of the fracture. The particle trajectories are overlain on a map that identifies regions that are smaller (blue) and larger (white) than the microcapsules. Particle blocking on a local scale can occur in regions where the aperture is larger than the microcapsules as shown by the significant blockage that developed in the bottom righthand corner of the fracture (Figure 8a).

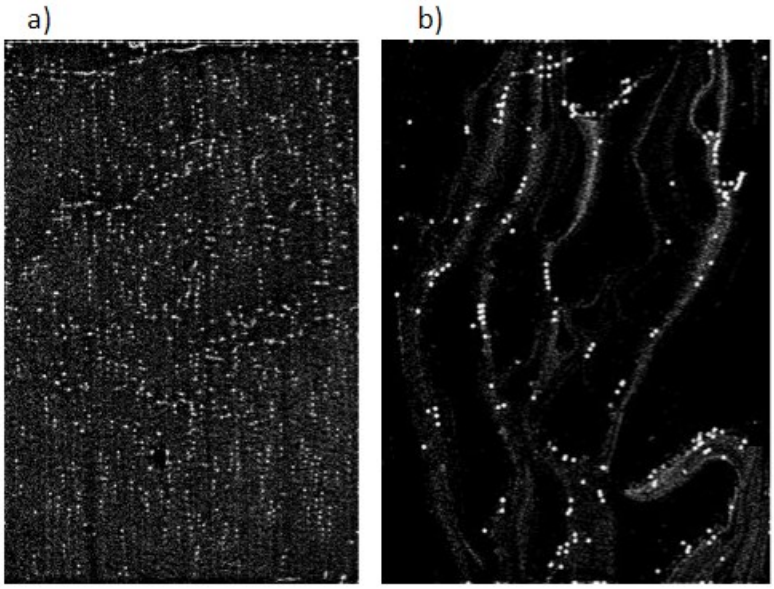

Figure 8 – (a) Particle trajectories for normally displaced fracture revealing parallel flow paths over the entire fracture surface. 0.5 mm microcapsules were used and the fracture was displaced 1 mm. (b) Particle trajectories for sheared fracture displaying tortuous flow concentrated in channels and excluded from large portions of the fracture. 1 mm diameter microcapsules were used in the fracture which was sheared 3 mm. White dots are microcapsules moving in well-connected flow paths.

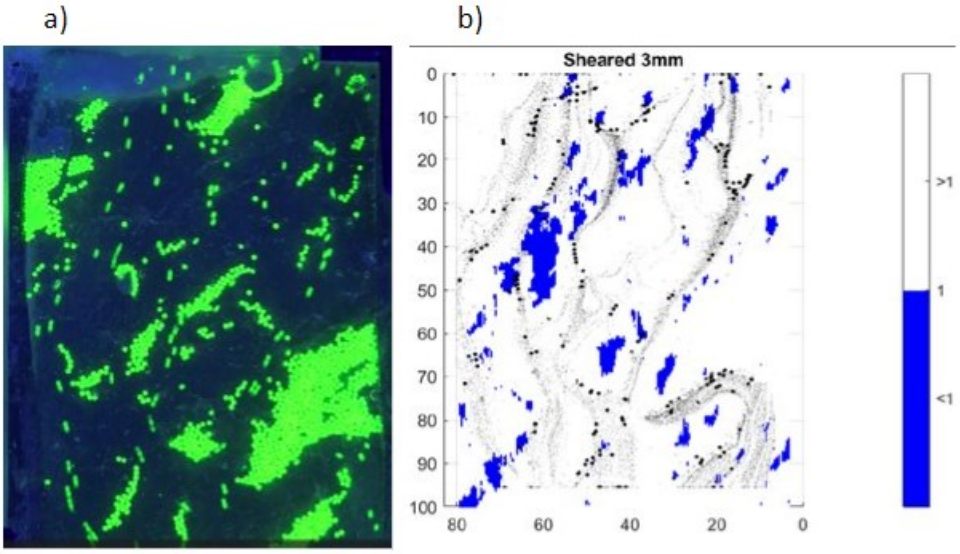

Figure 9 - (a) Photograph at conclusion of flow test in sheared sample revealing blocked area. (b) Particle trajectories in same fracture showing continuous flow through the fracture in spite of significant blockage. The particle trajectories are overlain on a fracture aperture map which identifies regions in blue that are smaller than the microcapsule size.

CONCLUSIONS

Microcapsules are being evaluated to deliver materials to modify fracture permeability in EGS. Understanding the movement of the microcapsules into variably sized rough fractures is a key challenge for successful deployment of this technology.

We have developed a flow visualization system to investigate controls on microcapsule movement and blockage during transport in rough fractures. Photographs and videos from the tests were interpreted to determine the amount of fracture blocking that occurs and the trajectories of the microcapsules within the fracture. Our preliminary tests indicate that:

Significant blocking of normally displaced fractures occurs when relative size of the fracture aperture to that of the microcapsule is less than 2, which is a smaller value than many existing conventional blocking criteria developed for other materials under different conditions.

Flow in sheared fractures is more complicated, resulting in tortuous and channelized flow. Microcapsule flow is channelized into the larger flow paths and excluded from locations with apertures less the microcapsule size.

Ongoing testing involves different sizes and types of microcapsules and microcapsule densities, fracture topographies, and flow rates.

ACKNOWLEDGEMENT

This material is based upon work supported by the U.S. Department of Energy's Office of Energy Efficiency and Renewable Energy (EERE) under the Geothermal Technologies Office, Award Number DE-EE0009787. The view expressed herein do not necessarily represent the view of the U.S. Department of Energy or the United States Government.

REFERENCES

Axelsson, M., Gustafson, G., Fransson, Å., 2009. Stop mechanism for cementitious grouts at different water-to-cement ratios. Tunneling Undergr. Space Technol. 24, 390–397. https://doi.org/10.1016/j.tust.2008.11.001

Develi, K., Babadagli, T., 2015. Experimental and visual analysis of single-phase flow through rough fracture replicas. Int. J. Rock Mech. Min. Sci. 73, 139–155. https://doi.org/10.1016/j.ijrmms.2014.11.002

Dontsov, E.V., Peirce, A.P., 2015. Proppant transport in hydraulic fracturing: Crack tip screen-out in KGD and P3D models. Int. J. Solids Struct. 63, 206–218. https://doi.org/10.1016/j.ijsolstr.2015.02.051

Eklund, D., Stille, H., 2008. Penetrability due to filtration tendency of cement-based grouts. Tunn. Undergr. Space Technol. 23, 389–398. https://doi.org/10.1016/j.tust.2007.06.011

Isakov, E., Ogilvie, S.R., Taylor, C.W., Glover, P.W.J., 2001. Fluid flow through rough fractures in rocks I: high resolution aperture determinations. Earth Planet. Sci. Lett. 191, 267–282. https://doi.org/10.1016/S0012-821X(01)00424-1

Jang, H.-S., Kang, S.-S., Jang, B.-A., 2014. Determination of Joint Roughness Coefficients Using Roughness Parameters. Rock Mech. Rock Eng. 47, 2061–2073. https://doi.org/10.1007/s00603-013-0535-z

Naets, I., Ahkami, M., Huang, P.-W., Saar, M.O., Kong, X.-Z., 2022. Shear induced fluid flow path evolution in rough-wall fractures: A particle image velocimetry examination. J. Hydrol. 610, 127793. https://doi.org/10.1016/j.jhydrol.2022.127793

Patterson, J.R., Cardiff, M., Feigl, K.L., 2020. Optimizing geothermal production in fractured rock reservoirs under uncertainty. Geothermics 88, 101906. https://doi.org/10.1016/j.geothermics.2020.101906

Roy, P., Walsh, S.D.C., Du Frane, W.L., Vericella, J.J., Smith, W.L., Stolaroff, J.K., Smith, M.M., Duoss, E.B., Spadaccini, C.M., Bourcier, W.L., Carroll, S., Roberts, J.J., Aines, R.D., 2015. Fabrication and Transport of Double Emulsion Microcapsules for Applications in Unconventional Resources. Presented at the SPE/AAPG/SEG Unconventional Resources Technology Conference, OnePetro. https://doi.org/10.15530/URTEC-2015-2154212

Witherspoon, P.A., Wang, J.S.Y., Iwai, K., Gale, J.E., 1980. Validity of Cubic Law for fluid flow in a deformable rock fracture. Water Resour. Res. 16, 1016–1024. https://doi.org/10.1029/WR016i006p01016